

## The modified cumulant expansion for two-dimensional isotropic turbulence

By TOMOMASA TATSUMI AND SHINICHIRO YANASE†

Department of Physics, Faculty of Science, University of Kyoto, Kyoto 606, Japan

(Received 4 January 1980 and in revised form 9 February 1981)

The two-dimensional isotropic turbulence in an incompressible fluid is investigated using the modified zero fourth-order cumulant approximation. The dynamical equation for the energy spectrum obtained under this approximation is solved numerically and the similarity laws governing the solution in the energy-containing and enstrophy-dissipation ranges are derived analytically. At large Reynolds numbers the numerical solutions yield the  $k^{-3}$  inertial subrange spectrum which was predicted by Kraichnan (1967), Leith (1968) and Batchelor (1969) assuming a finite enstrophy dissipation in the inviscid limit. The energy-containing range is found to satisfy an inviscid similarity while the enstrophy-dissipation range is governed by the quasi-equilibrium similarity with respect to the enstrophy dissipation as proposed by Batchelor (1969). There exists a critical time  $t_c$  which separates the initial period ( $t < t_c$ ) and the similarity period ( $t > t_c$ ) in which the enstrophy dissipation vanishes and remains non-zero respectively in the inviscid limit. Unlike the case of three-dimensional turbulence,  $t_c$  is not fixed but increases indefinitely as the viscosity tends to zero.

---

### 1. Introduction

Two-dimensional isotropic turbulence is a highly idealized version of turbulent fluid motion. It has attracted the interest of researchers owing to its relevance to the atmospheric circulation at intermediate scale and to magnetohydrodynamic motions with strong magnetic fields. An obvious feature of two-dimensional turbulence is that the mean-squared vorticity (or enstrophy) is an inviscid invariant, as well as the energy which is also invariant for inviscid three-dimensional flows. The existence of this extra invariant makes the statistical properties of two-dimensional turbulence entirely different from those of more familiar three-dimensional turbulence. A typical consequence is the presence of a strong energy transfer from higher to lower wavenumbers which leads to the vanishing energy dissipation in the inviscid limit. Another consequence is the forward enstrophy transfer from lower to higher wavenumbers just like the energy transfer in three-dimensional turbulence.

The existence of energy transfer from small-scale components to large-scale ones was already noted in the classical work by Onsager (1949), which describes the gathering of vortices of the same sense and the dispersion of vortices of the opposite sense. The corresponding energy transfer from higher to lower wavenumbers was first

† Present address: Engineering Mathematics, School of Engineering, Okayama University, Okayama 700, Japan.

explicitly mentioned by Fjørtoft (1953) who found that only a small fraction of the energy flows to higher wavenumbers while a greater fraction flows to lower wavenumbers. The same trend was also observed in the numerical calculation of the energy spectrum by Ogura (1962) based upon the zero fourth-order cumulant approximation, but the calculation was interrupted by the occurrence of negative values of the energy spectrum.

The simultaneous existence of the energy and enstrophy transfer processes in two-dimensional turbulence was first noted by Kraichnan (1967), and it was predicted that the  $k^{-5/3}$  spectrum is associated with the backward energy transfer and the  $k^{-3}$  spectrum, modified by a logarithmic factor, is associated with the forward enstrophy transfer. In a subsequent paper, Kraichnan (1971) determined the logarithmic factor explicitly. Leith (1968) also derived the  $k^{-3}$  spectrum using a simple diffusion model. An explicit use of the notion of the enstrophy transfer was made by Batchelor (1969) who derived a similarity form of the energy spectrum for the equilibrium range, which yields the  $k^{-3}$  spectrum in the inertial subrange, using a similar argument to Kolmogorov's for three-dimensional turbulence. He also derived a similarity law of the energy spectrum for the energy-containing range assuming that the energy-containing and enstrophy-containing ranges obey the same similarity law.

Two-dimensional turbulence has been dealt with by several authors using various closure assumptions. Leith (1971) carried out a numerical calculation of the energy spectrum based upon the Markovian eddy-damped approximation and obtained the  $k^{-3}$  spectrum. Later the calculation was extended by Pouquet *et al.* (1975) to the time-dependent case at much higher Reynolds numbers taking account of the effect of non-local interactions between different wavenumber components, and the same spectrum was obtained. Kraichnan (1971) determined the numerical factor of the  $k^{-3}$  spectrum using the test field model, and the  $k^{-3}$  spectrum was obtained from a numerical calculation by Leith & Kraichnan (1972) based on the same model. Leith (1971) and Leith & Kraichnan (1972) analysed the growth of the initial uncertainty in the atmospheric motions applying the notion of the backward energy transfer in two-dimensional turbulence and discussed the predictability of such motions. A different type of the spectrum which is proportional to  $k^{-4}$  was proposed by Saffman (1971) using a conjecture that the vorticity field of two-dimensional turbulence will take a piece-wise continuous pattern just like the piece-wise continuous velocity field of Burgers turbulence.

As stated above, the  $k^{-3}$  inertial subrange spectrum is based upon the existence of non-zero enstrophy flux in the inviscid limit, while the  $k^{-4}$  spectrum is associated with the vanishing enstrophy flux in this limit. Now it was proved by Pouquet *et al.* (1975) under the Markovian eddy-damped approximation that the enstrophy dissipation vanishes with the viscosity at any finite time. This conclusion seems to conflict with the existence of the  $k^{-3}$  spectrum, which was also obtained by their numerical calculation using the same assumption. It will be shown below, however, that no contradiction exists since the conclusion of Pouquet *et al.* only requires that it takes increasingly longer time as the viscosity decreases before the  $k^{-3}$  spectrum is realized.

In the present paper, two-dimensional isotropic turbulence in an incompressible fluid is investigated by applying the modified zero fourth-order cumulant approximation used by Tatsumi & Kida (1980) for three-dimensional isotropic turbulence. Although this approximation is the lowest-order approximation in both the cumulant

expansion and Taylor expansion of the memory integral, the similarity laws derived from this approximation are shown to be exact by taking account of higher-order approximation.

In §2, the equation governing the energy spectrum of two-dimensional turbulence is derived using this approximation. In §3, the general properties of two-dimensional turbulence are discussed with particular reference to the possibility of the  $k^{-3}$  spectrum. §4 describes the procedure in the numerical calculation, and its results are presented in detail in §5. In §6, the similarity laws in different wavenumber ranges are derived analytically from the energy spectrum equation and their validity is examined by comparing with numerical results. §7 describes the decay of enstrophy and its similarity laws. In §8, the similarity laws governing the higher-order cumulants and characteristic functional are derived, and it is shown that some part of the similarity laws obtained in §§6 and 7 are exact results independent of any closure assumption. Finally, the comparative discussion of the present results with those obtained from numerical experiments is made in §9.

## 2. Equation for the energy spectrum

The two-dimensional motions in an incompressible viscous fluid are expressed in terms of either the velocity  $\mathbf{u}(\mathbf{x}, t) = (u_1, u_2)$  or the vorticity  $\omega(\mathbf{x}, t) = \partial u_1/\partial x_2 - \partial u_2/\partial x_1$  as a function of the two-dimensional rectangular co-ordinates  $\mathbf{x} = (x_1, x_2)$  and the time  $t$ . The vorticity  $\omega(\mathbf{x}, t)$  is governed by the following equation:

$$\frac{\partial \omega}{\partial t} + \frac{\partial(\omega, \psi)}{\partial(x_1, x_2)} = \nu \Delta \omega, \quad \omega = -\Delta \psi, \quad (2.1)$$

where  $\psi(\mathbf{x}, t)$  is the stream function,  $\nu$  the kinematic viscosity and  $\Delta \equiv \partial^2/\partial x_1^2 + \partial^2/\partial x_2^2$ .

Two-dimensional homogeneous turbulence is described completely by the characteristic functional of the probability distribution of Fourier-transformed vorticity

$$\chi(\mathbf{k}, t) = \frac{1}{(2\pi)^2} \int \omega(\mathbf{x}, t) \exp(-i\mathbf{k} \cdot \mathbf{x}) d\mathbf{x}, \quad (2.2)$$

where  $\mathbf{k} = (k_1, k_2)$  is the two-dimensional wavenumber vector. The characteristic functional is defined by

$$\Phi[z(\mathbf{k}), t] \equiv \langle \exp[i(z, \chi)] \rangle, \quad (z, \chi) \equiv \int z^*(\mathbf{k}) \chi(\mathbf{k}, t) d\mathbf{k}, \quad (2.3)$$

where  $\langle \rangle$  denotes the mean value with respect to the probability distribution of  $\chi(\mathbf{k}, t)$ ,  $*$  the complex conjugate and  $z(\mathbf{k})$  an arbitrary argument function of  $\mathbf{k}$ . The equation for  $\Phi[z, t]$  is derived from the law of conservation of the probability and equation (2.1) as follows:

$$\frac{\partial \Phi}{\partial t} + \nu \int k^2 z^*(\mathbf{k}) \frac{\delta \Phi}{\delta z^*(\mathbf{k})} d\mathbf{k} = -i \iint \frac{k'_1 k_2 - k'_2 k_1}{|\mathbf{k} - \mathbf{k}'|^2} z^*(\mathbf{k}) \frac{\delta^2 \Phi}{\delta z^*(\mathbf{k}') \delta z^*(\mathbf{k} - \mathbf{k}')} d\mathbf{k} d\mathbf{k}', \quad (2.4)$$

where  $\delta/\delta z(\mathbf{k})$  denotes the functional derivative.

The cumulants of the probability distribution,  $C^{(n)}$  ( $n = 1, 2, \dots$ ) say, are defined as the coefficients of the logarithmic Taylor expansion of  $\Phi[z, t]$ . For isotropic turbulence, the mean vorticity vanishes identically so that  $C^{(1)} = 0$ . Using the lowest-order approximation of the modified cumulant expansion, we obtain from (2.4) the equation for  $C^{(2)}$ .

For isotropic turbulence,  $C^{(2)}$  may be written in terms of the energy spectrum function  $E(k, t)$ , where  $k = |\mathbf{k}|$ . Thus, the equation for  $C^{(2)}$  yields the following equation for  $E(k, t)$ :

$$\left. \begin{aligned} \left(\frac{\partial}{\partial t} + 2\nu k^2\right) E(k, t) &= T(k, t), \\ T(k, t) &= \frac{4k}{\pi} \int_0^\infty dk' \int_{-1}^1 \theta(t) [kE(k') - k'E(k)] E(k'') \left(\frac{kk'}{k''^2} + 2\mu\right) \frac{k'}{k''} (1 - \mu^2)^{\frac{1}{2}} d\mu, \\ \theta(t) &= \frac{1 - \exp[-\nu(k^2 + k'^2 + k''^2)t]}{\nu(k^2 + k'^2 + k''^2)}, \end{aligned} \right\} \quad (2.5)$$

where  $k''^2 = k^2 + k'^2 + 2\mu kk'$ ,  $T(k, t)$  is the energy transfer function and the initial condition

$$T(k, 0) = 0 \tag{2.6}$$

has been assumed.

If the energy spectrum  $E(k, t)$  is known, the energy, the enstrophy and the palinstrophy are expressed in terms of  $E(k, t)$  as follows:

$$\left. \begin{aligned} \text{Energy} \quad \mathcal{E}(t) &= \frac{1}{2} \langle |\mathbf{u}|^2 \rangle = \int_0^\infty E(k, t) dk, \\ \text{Enstrophy} \quad \mathcal{Q}(t) &= \frac{1}{2} \langle \omega^2 \rangle = \int_0^\infty k^2 E(k, t) dk, \\ \text{Palinstrophy} \quad \mathcal{P}(t) &= \frac{1}{2} \langle |\text{rot } \boldsymbol{\omega}|^2 \rangle = \int_0^\infty k^4 E(k, t) dk, \end{aligned} \right\} \quad (2.7)$$

where  $\boldsymbol{\omega} = (0, 0, \omega)$ .

### 3. General properties of two-dimensional turbulence

For two-dimensional flows in viscous fluid, the energy  $\mathcal{E}$  and the enstrophy  $\mathcal{Q}$  decay in time, and the rates of their dissipation are given from (2.1) as

$$\epsilon(t) \equiv -\frac{d}{dt} \mathcal{E}(t) = 2\nu \mathcal{Q}(t). \tag{3.1}$$

$$\eta(t) \equiv -\frac{d}{dt} \mathcal{Q}(t) = 2\nu \mathcal{P}(t). \tag{3.2}$$

Equation (3.1) also holds for three-dimensional fluid motions.

In the case of three-dimensional turbulence, it is generally accepted that the energy dissipation remains non-zero in the limit of vanishing viscosity:

$$\epsilon > 0 \quad \text{as} \quad \nu \rightarrow 0 \tag{3.3}$$

(see Proudman & Reid 1954; Brissaud *et al.* 1973; André & Lesieur 1977; Orszag 1977; Tatsumi, Kida & Mizushima 1978). The relationship (3.3) implies that

$$\mathcal{Q} \rightarrow \infty \quad \text{as} \quad \nu \rightarrow 0, \tag{3.4}$$

that is, an enstrophy catastrophe occurs in this limit.

For two-dimensional turbulence on the other hand, the enstrophy catastrophe does not occur since it follows from (3.1) and (3.2) that

$$\epsilon \rightarrow 0 \quad \text{as} \quad \nu \rightarrow 0. \tag{3.5}$$

Therefore Kolmogorov's hypothesis is not applicable to two-dimensional turbulence and the  $k^{-5/3}$  spectrum does not necessarily hold for this turbulence. (When an external energy supply is present, the  $k^{-5/3}$  spectrum may exist on account of the independence of the rate of energy supply from the viscosity.)

On the other hand, the possibility of non-zero enstrophy dissipation in the inviscid limit,

$$\eta > 0 \quad \text{as} \quad \nu \rightarrow 0, \tag{3.6}$$

is not excluded since the palinstrophy  $\mathcal{P}$  may increase indefinitely even in two-dimensional flows. Batchelor (1969) proposed to adopt (3.6) as the basic hypothesis for two-dimensional turbulence and, assuming the quasi-equilibrium of enstrophy, derived the following similarity form of the energy spectrum:

$$\left. \begin{aligned} E(k,t) &= \eta^{1/2} \nu^{3/2} E_e(k/k_d), \\ k_d &= \eta^{1/2} \nu^{-1/2} \end{aligned} \right\} \tag{3.7}$$

for  $k \approx k_d \gg k_0$ , where  $k_0$  and  $k_d$  are the wavenumbers characterizing the energy-containing and enstrophy-dissipation ranges respectively and  $E_e$  is a non-dimensional function. If the Reynolds number is large enough, there appears an inertial subrange where the spectrum becomes independent of  $\nu$  and (3.7) reduces to

$$E(k) = C \eta^{2/3} k^{-3}, \tag{3.8}$$

where  $C$  is a non-dimensional constant.

It was shown by Pouquet *et al.* (1975) using the Markovian eddy-damped approximation, which includes the present approximation as a limiting case, that

$$\mathcal{P}(t) < \mathcal{P}(0) \exp \left[ \frac{1}{2} \mathcal{Q}(0) t^2 \right], \tag{3.9}$$

and hence that  $\mathcal{P}(t)$  remains finite at any finite time. Then it follows from (3.2) that

$$\eta \rightarrow 0 \quad \text{as} \quad \nu \rightarrow 0 \tag{3.10}$$

for finite  $t$ . This result is in apparent contradiction with the assumption (3.5), but this contradiction will be resolved later on by noticing the non-uniform character of the limiting processes  $\nu \rightarrow 0$  and  $t \rightarrow \infty$ .

Lastly let us examine the possibility of an absolute equilibrium state for two-dimensional turbulence in the inviscid limit  $\nu \rightarrow 0$ . The canonical distribution for two-dimensional turbulence was discussed in detail by Kraichnan (1967, 1975). The energy spectrum associated with this distribution is given by

$$E(k) = \frac{k}{a + bk^2}, \tag{3.11}$$

where  $a$  and  $b$  are constants corresponding to the inviscid invariants  $\mathcal{E}$  and  $\mathcal{Q}$ . The canonical spectrum (3.11) represents the equipartition of energy at lower wavenumbers and the enstrophy equipartition at higher wavenumbers. The spectrum (3.11) is also obtained as a stationary solution of the equation  $T(k,t) = 0$ , to which the energy spectrum equation (2.5) reduces for an identically inviscid fluid  $\nu = 0$ .

It should be remembered, however, that the canonical distribution and the spectrum (3.11) are not applicable to the real two-dimensional turbulence since, as will be shown later, the effect of the viscous dissipation cannot be neglected even in the limit of vanishing viscosity. The situation becomes quite different if we consider a model turbulence which has only finite wavenumbers truncated at a large but finite value. In the inviscid limit, such a model turbulence becomes an isolated system with the two inviscid invariants  $\mathcal{E}$  and  $\mathcal{Q}$  and the canonical distribution is realizable for this model system.

Numerical experiments on such model systems have been carried out by several authors (Fox & Orszag 1973; Basdevant & Sadourny 1975; Seyler *et al.* 1975; Kells & Orszag 1978). Numerical results obtained all show rapid approach of the energy spectrum toward the canonical spectrum (3.11). Thus, the absolute equilibrium state characterized by (3.11) is realizable for two-dimensional systems having finite wavenumbers. On the other hand, the numerical simulation by Fornberg (1977) which also deals with an inviscid truncated system but one provided with an artificial energy sink at the highest wavenumber clearly shows the approach to the inertial subrange spectrum (3.8). A comprehensive discussion of the two-dimensional inertial subrange may be found in a review by Kraichnan & Montgomery (1979).

#### 4. Numerical calculation

For the convenience of numerical work all variables are made non-dimensional with respect to the representative wavenumber  $k_0$  and velocity  $u_0$  of turbulence:

$$\text{wavenumber } \kappa = k/k_0, \quad \text{time } \tau = u_0 k_0 t, \quad \text{Reynolds number } R = u_0/(\nu k_0). \quad (4.1)$$

As the initial condition the following two cases are considered:

$$\text{(I)} \quad E(k, 0)/E_0 = 2(k/k_0) \exp(-k^2/k_0^2), \quad (4.2)$$

$$\text{(II)} \quad E(k, 0)/E_0 = 2(k/k_0)^3 \exp(-k^2/k_0^2), \quad (4.3)$$

where  $E_0 = u_0^2/k_0$ . Cases I and II represent the initial states in which the energy spectrum density  $E(k)/2\pi k$  is non-zero and zero respectively at zero wavenumber.

The energy spectrum equation (2.5) is solved numerically for the initial conditions (4.2) and (4.3) and Reynolds numbers  $R = 20, 100, 200, 400, 10^4$  and  $10^5$ . The integration with respect to  $k'$  is carried out using Simpson's sum rule with uneven mesh sizes  $\kappa' = k'/k_0 = ab^n$ ,  $a = 0.1$ ,  $b = 1.11 \sim 1.14$ ,  $n = 1, 2, \dots, N$ , and  $N = 40 \sim 75$ , where smaller  $b$  and larger  $N$  are used for larger values of  $R$ . The integration with respect to  $\mu$  is made using the 40-point Legendre-Gauss method which employs variable mesh sizes, finer around  $\mu \approx \pm 1$  than around  $\mu \approx 0$ . The time integration is made by the forward difference method with the increment  $\Delta\tau = 0.01$ .

Statistical quantities such as the energy  $\mathcal{E}(t)$ , the enstrophy  $\mathcal{Q}(t)$  and the palinstrophy  $\mathcal{P}(t)$  are derived from (2.7) using the numerical result of the energy spectrum  $E(k, t)$ .

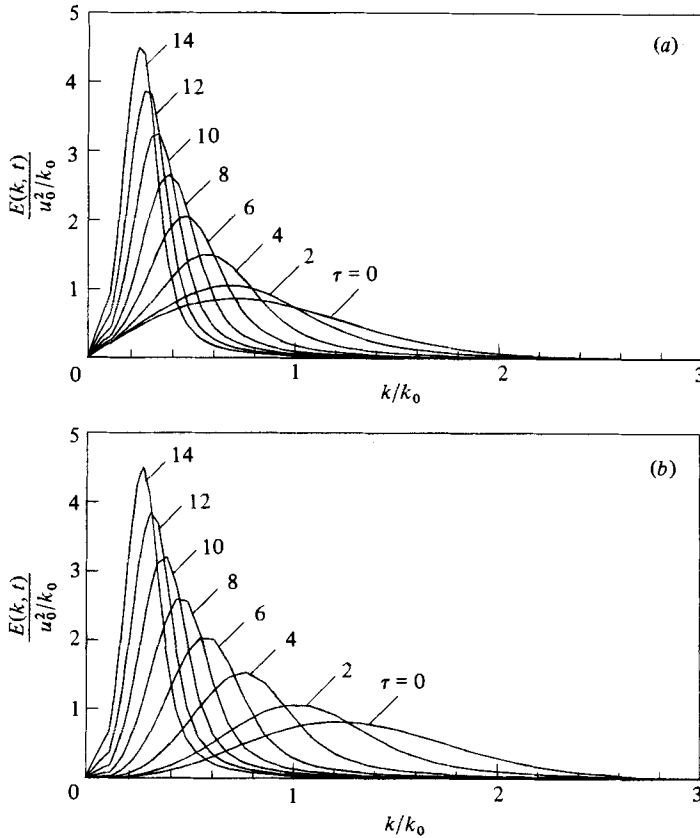


FIGURE 1. The energy spectrum function  $E(k, t)$  for  $R = 10^5$ . (a) Case I. (b) Case II.

### 5. Energy spectrum

The evolution of the energy spectrum  $E(k, t)$  for  $R = 10^5$  is shown graphically in figures 1 and 2. In contrast to three-dimensional turbulence, there exists a strong energy transfer from higher to lower wavenumbers. This backward energy transfer towards the region of vanishing viscous effect is actually responsible for the conservation of energy  $\mathcal{E}(t)$  for two-dimensional turbulence at large Reynolds numbers.

It may be seen in figure 2 that the energy spectrum satisfies a similarity law over a finite wavenumber range. The similarity is confirmed by making curves of  $E(k, t)$  for different Reynolds numbers and times coincide with each other. For large Reynolds numbers, there are found to exist two similarity regions corresponding to the energy-containing and enstrophy-dissipation ranges.

#### (i) Energy-containing range

The energy-containing ranges of the spectra for  $R = 400$ ,  $10^4$  and  $10^5$  and different times are put together to make a similarity curve as shown in figure 3. For case I, the similarity does not cover very low wavenumbers, and the gradient of  $E(k, t)$  increases in time from 1 at  $\tau = 0$  to 2 at  $\tau = 14$ . For case II, on the other hand, the similarity is satisfied perfectly down to zero wavenumber and this fact is consistent with the

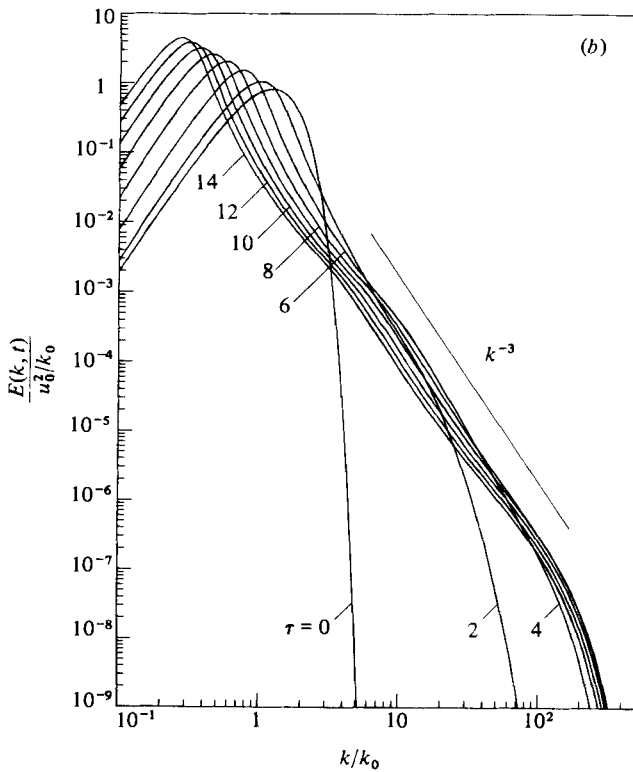
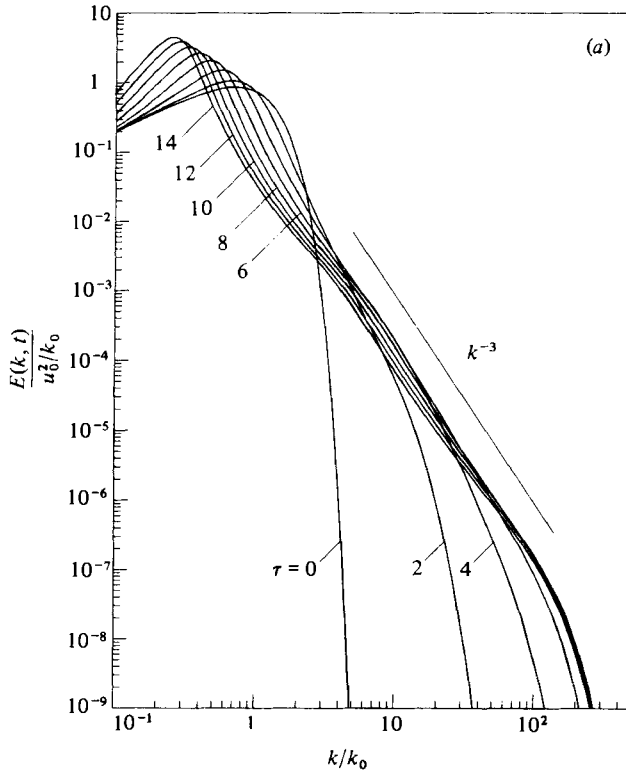


FIGURE 2. The energy spectrum function  $E(k,t)$  with a logarithmic scale. (a) Case I. (b) Case II.



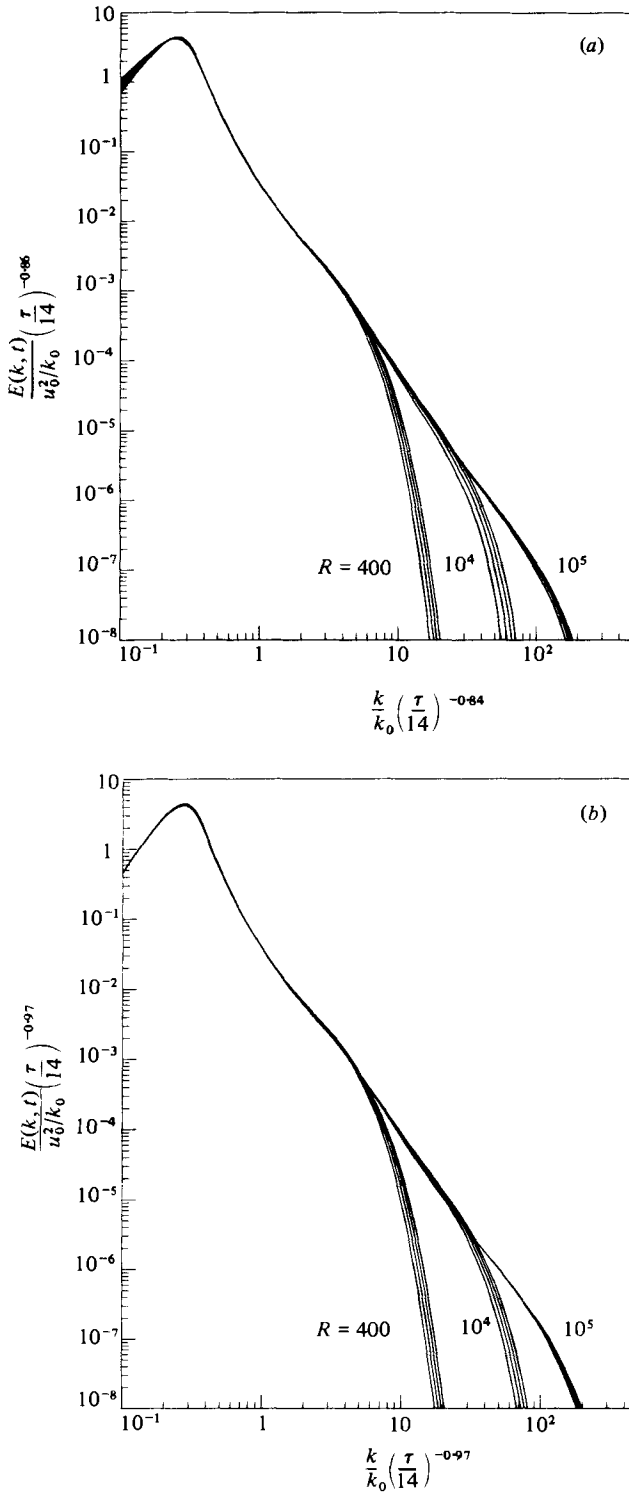


FIGURE 3. The similarity of the energy spectrum function  $E(k, t)$  in the energy-containing range. (a) Case I. (b) Case II.

analytical result which will be given in §6 that the similarity spectrum has the form  $E(k, t) \propto k^3$  at  $k \approx 0$ . The similarity form in the energy-containing range is found to be independent of Reynolds number  $R$  and its time similarity is expressed as

$$E(k, t)/E_0 = \begin{cases} \tau^{0.86} F(\kappa\tau^{0.84}) & \text{for case I,} \\ \tau^{0.97} F(\kappa\tau^{0.97}) & \text{for case II,} \end{cases} \quad (5.1)$$

where  $F$  is a non-dimensional function.

The similarity spectra for large Reynolds numbers  $R = 10^4$  and  $10^5$  have a common inverse power region as follows:

$$E(k, t)/E_0 = \begin{pmatrix} 13.6 \\ 12.4 \end{pmatrix} \tau^{-2} \kappa^{-3} \begin{cases} \text{for case I,} \\ \text{for case II,} \end{cases} \quad (5.2)$$

where the coefficients have been determined from the superimposed curves. The existence of the  $k^{-3}$  spectrum in the numerical results indicates that the present approximation is compatible with the notion of non-zero enstrophy dissipation (3.6) in the inviscid limit.

#### (ii) *Enstrophy-dissipation range*

Unlike the energy-containing range, the spectral curves obtained do not satisfy any definite time-similarity in this range but obey a similarity with respect to Reynolds number, which may be expressed for curves at  $\tau = 10$  and  $R = 10^4$  and  $10^5$  as

$$E(k, t)/E_0 = \begin{cases} R^{-1.53} F(\kappa/R^{0.51}) & \text{for case I,} \\ R^{-1.32} F(\kappa/R^{0.45}) & \text{for case II.} \end{cases} \quad (5.3)$$

It is interesting to note that the exponents of  $R$  ( $\propto \nu^{-1}$ ) given above are in fairly good agreement with those of (3.7) based on the quasi-equilibrium of enstrophy.

Although the spectral curves do not satisfy a single similarity law, the curves for  $R \geq 10^4$  become proportional to  $k^{-3}$  at lower wavenumbers in this range. At higher wavenumbers, on the other hand, the spectrum takes the following exponential form:

$$E(k, t) \propto \exp(-b\kappa^s), \quad (5.4)$$

where  $s = 1.3 \sim 1.4$  and  $b$  is a constant. It will be shown, however, in §6 that  $s \simeq 1$  as  $k \rightarrow \infty$ . This discrepancy indicates that either the asymptotic behaviour  $s \simeq 1$  is realized beyond the numerical coverage or the numerical results are not accurate enough, but anyway the latter possibility cannot be ignored. In either case, the asymptotic form of the spectrum is different from the purely viscous spectrum,

$$E(k, t) \propto \exp(-2\nu k^2 t), \quad (5.5)$$

which is characteristic of weak turbulence. Thus it is concluded that the nonlinear inertial effect cannot be neglected even at very high wavenumbers where the spectral intensity is very low.

## 6. Similarity laws for the energy spectrum

The similarity form of the energy spectrum with respect to Reynolds number and time is expressed as

$$E(k, t)/E_0 = R^\alpha \tau^\beta F(\kappa/(R^\gamma \tau^\delta)), \quad (6.1)$$

where  $\alpha, \beta, \gamma$  and  $\delta$  are constants and  $F$  is a non-dimensional function. These exponents and function have been determined numerically in §5, but the exponents can also be obtained analytically by solving the energy spectrum equation in the respective wave-number ranges.

Similarity arguments concerning the energy spectrum have already been put forward for three-dimensional turbulence. Lesieur & Schertzer (1978) analysed the similarity laws using the Markovian eddy-damped approximation and examined the dependence of the energy decay law on the structure of the spectrum at very low wavenumbers. Tatsumi & Kida (1980) showed, using the modified zero fourth-cumulant approximation, that there exist three similarity laws corresponding to the energy-containing, intermediate and energy-dissipation ranges and concluded that the similarity exponents for the first and last ranges are exact values uninfluenced by taking account of higher-order cumulants.

For two-dimensional turbulence, there exist only two similarity ranges, corresponding to the energy-containing and enstrophy-dissipation ranges.

(i) *Energy-containing range*

The energy-containing range is characterized by

$$k \approx k_0. \tag{6.2}$$

In the inviscid limit  $\nu \rightarrow 0$ , the energy spectrum equation (2.5) takes the following form in this range:

$$\frac{\partial E(k, t)}{\partial t} = \frac{4kt}{\pi} \int_0^\infty dk' \int_{-1}^1 [kE(k', t) - k'E(k, t)] E(k'', t) \left( \frac{kk'}{k''^2} + 2\mu \right) \frac{k'}{k''} (1 - \mu^2)^{\frac{1}{2}} d\mu. \tag{6.3}$$

It immediately follows from the Reynolds number independence of (6.3) that

$$\alpha = \gamma = 0. \tag{6.4}$$

Substituting (6.1) with (6.4) into (6.3) and equating powers of  $\tau$  on both sides, we obtain

$$\beta + 3\delta = -2. \tag{6.5}$$

Another relation follows from the invariance of the energy  $\mathcal{E}$ , which is written, on substitution from (6.1), as

$$\mathcal{E} = \tau^{\beta+\delta} \int_0^\infty F(s) ds = \text{const.}, \tag{6.6}$$

so that

$$\beta + \delta = 0. \tag{6.7}$$

Hence it follows from (6.5) and (6.7) that

$$\beta = -\delta = 1. \tag{6.8}$$

With the exponents (6.4) and (6.8), the similarity form (6.1) is written as

$$E(k, t)/E_0 = \tau F(\kappa\tau). \tag{6.9}$$

This analytical form is in good agreement with numerical result (5.1) for case II but less accurately with that for case I. The similarity form (6.9) was first derived by Batchelor (1969) from dimensional analysis based on the conservation of energy.

The expression (6.9) enables us to obtain the law of evolution of the enstrophy if it is assumed to be determined by the energy spectrum in the energy-containing range. Substitution of (6.9) into (2.7) immediately gives

$$\mathcal{Q}(t) = (u_0 k_0)^2 J \tau^{-2}, \quad (6.10)$$

so that, from (3.2),

$$\eta(t) = 2(u_0 k_0)^3 J \tau^{-3}, \quad (6.11)$$

where

$$J = \int_0^\infty s^2 F(s) ds. \quad (6.12)$$

The time dependence of these quantities was also obtained by Batchelor (1969) following the same argument. As a matter of fact, it will be shown in (ii) below that the enstrophy-dissipation range also makes a contribution to the enstrophy but its time dependence is not affected by this contribution.

The asymptotic form of the energy spectrum for very small wavenumbers can be obtained analytically. If we assume the spectrum for  $k \approx 0$  in the form

$$E(k, t)/E_0 = A_a(t) (k/k_0)^a, \quad (6.13)$$

$a$  being a positive constant and  $A_a$  a function of time in general, equation (6.3) is expressed, to the lowest order of  $k$ , as

$$\frac{dA_a(t)}{dt} = \frac{k_0^a}{E_0} k^{3-a} t \int_0^\infty E(k', t)^2 k'^{-1} dk'. \quad (6.14)$$

For  $a < 3$ , including case I ( $a = 1$ ), the right-hand side of (6.14) is of higher order of  $k$  than the left-hand side, so that  $dA_a/dt = 0$ , that is,

$$A_a = \text{const. for } a < 3. \quad (6.15)$$

The invariance of the gradient  $A_1$  of the energy spectrum for case I at small wavenumbers is not observable in the numerical curves shown in figure 2a, but must be present at still smaller wavenumbers.

For  $a = 3$ , on the other hand, (6.14) yields the solution

$$A_3(t) = \frac{k_0^3}{2E_0} t^2 \int_0^\infty E(k', t)^2 k'^{-1} dk' = \frac{1}{2} \tau^4 \int_0^\infty F(s)^2 s^{-1} ds, \quad (6.16)$$

in view of (6.9). Thus, the similarity form (6.9) is explicitly written at very small wavenumbers as

$$E(k, t)/E_0 = \frac{1}{2} \kappa^3 \tau^4 \int_0^\infty F(s)^2 s^{-1} ds. \quad (6.17)$$

The complete validity of the similarity (6.9) down to the region of very small wavenumbers is satisfied with good accuracy by numerical curves for case II ( $a = 3$ ) as shown in figure 3b. The  $k^3$  dependence of the energy spectrum for  $k \approx 0$  was first given by Basdevant *et al.* (1978) using the Markovian eddy-damped approximation.

#### (ii) Enstrophy-dissipation range

The enstrophy-dissipation range is characterized by the wavenumber  $k_d$  defined by (3.7), which may also be written as

$$k_d = (\nu t)^{-\frac{1}{2}}, \quad (6.18)$$

in view of (6.11). The relation (6.18) gives the exponents of the similarity form (6.1) as

$$\gamma = -\delta = \frac{1}{2}. \tag{6.19}$$

Substitution of (6.1) with (6.19) into (2.5) determines the remaining exponents as

$$\alpha = -\frac{3}{2}, \quad \beta = -\frac{1}{2}, \tag{6.20}$$

and shows that all terms of (2.5) remain of the same order of magnitude in this range.

With the exponents (6.19) and (6.20), the similarity form (6.1) is written as

$$E(k, t)/E_0 = R^{-\frac{1}{2}}\tau^{-\frac{1}{2}}F(\kappa/(R^{\frac{1}{2}}\tau^{-\frac{1}{2}})). \tag{6.21}$$

The Reynolds number similarity given by (6.21) is satisfied very well by the numerical result for case I but less accurately by that for case II. On the other hand, no clear time similarity is revealed by the numerical results probably on account of insufficient accuracy of the numerical work.

The enstrophy dissipation  $\eta(t)$  is expressed in terms of the energy spectrum through (3.2) and the integral (2.7). Substituting the similarity forms (6.9) for the energy-containing range and (6.21) for the enstrophy-dissipation range into the integral, we find that the enstrophy-dissipation range gives the dominant contribution,

$$\eta(t) \propto R^0\tau^{-3}, \tag{6.22}$$

which is in accordance with (6.11), whereas that from the energy-containing range is of smaller order  $O(R^{-1}\tau^{-4})$ . This justifies us in referring to the wavenumber range (3.7) (or (6.18)) as the enstrophy-dissipation range.

In view of (6.22), the similarity law (6.21) is identical with (3.7) derived from the hypothesis of the quasi-equilibrium of enstrophy. Thus, the hypothesis is confirmed under the framework of the present approximation.

Similarly the contributions to the energy  $\mathcal{E}(t)$  can be examined. Substituting the similarity forms for the energy-containing and enstrophy-dissipation ranges into the enstrophy integral (2.7), we see that the contribution from the former range is  $O(R^0\tau^0)$  while that from the latter is of smaller order  $O(R^{-1}\tau^{-1})$ . This again confirms the appropriateness of the term energy-containing range.

The situation is different for the enstrophy  $\mathcal{Q}(t)$ . Substitution of the similarity form (6.21) into the enstrophy integral (2.7) gives the contribution,

$$\mathcal{Q}(t) \propto R^0\tau^{-2}, \tag{6.23}$$

which is of exactly the same order of magnitude as the contribution from the energy-containing range (6.10). Thus, the enstrophy is contributed equally from the energy-containing and enstrophy-dissipation ranges with the similarity exponents as given by (6.10) or (6.23). However, the enstrophy is still expressed by (6.10) if the numerical coefficient  $J$  given by (6.12) is changed by taking account of the contribution from the latter range.

(iii) *Inertial subrange*

The inertial subrange is the common region of the energy-containing and enstrophy-dissipation ranges. Thus, the energy spectrum in this subrange must satisfy the

similarity laws (6.9) for the former range and (6.21) for the latter simultaneously. This can be achieved only by the following similarity form:

$$E(k, t)/E_0 = C' \tau^{-2} \kappa^{-3}, \quad (6.24)$$

where  $C'$  is a non-dimensional constant. In view of the relation (6.21), this is nothing but the two-dimensional inertial subrange spectrum (3.8) obtained by Kraichnan (1967), Leith (1968) and Batchelor (1969) using the notion of the enstrophy cascade.

The numerical value of  $C'$  is determined from the curves of the energy spectrum for  $R = 10^5$  as

$$C' = \begin{cases} 13.6 & \text{for case I,} \\ 12.4 & \text{for case II,} \end{cases} \quad (6.25)$$

which are nearly equal to each other. The constant  $C$  of (3.8) can be calculated from (6.11) and (6.25) taking account of the contribution from the enstrophy-dissipation range, but this was not practicable due to the lack of time similarity of numerical data of the enstrophy-dissipation range.

(iv) *Logarithmic correction of time*

As is well known, the  $k^{-3}$  spectrum (6.24) gives rise to a divergent enstrophy (Kraichnan 1967, 1971; Pouquet *et al.* 1975). The enstrophy integral is evaluated using (6.9), (6.18) and (6.24) as

$$\mathcal{Q}(t) \approx \int_0^{k_d} k^2 E(k, t) dk \approx \tau^{-2} \log(R\tau), \quad (6.26)$$

so that

$$\eta(t) \approx \tau^{-3} \log(R\tau) \quad (6.27)$$

for large  $R$ . Hence, the enstrophy dissipation becomes

$$\eta \approx \log(1/\nu) \rightarrow \infty \quad \text{as} \quad \nu \rightarrow 0. \quad (6.28)$$

Obviously, the similarity law (6.21) is not consistent with (6.28) since the corresponding enstrophy dissipation (6.22) is of smaller order than (6.27). The consistency, however, can be restored by simply replacing the time  $\tau$  in (6.21) by

$$\tau_* = \tau [\log(R\tau)]^{-\frac{1}{3}}, \quad (6.29)$$

where the exponent  $-\frac{1}{3}$  of the logarithmic factor has been determined by requiring the balance of the dominant terms in (2.5) and the compatibility of the enstrophy-dissipation integral with (6.27). The logarithmic correction (6.29) yields the enstrophy of  $O(\tau^{-2}(\log(R\tau))^{\frac{2}{3}})$ , which is of smaller order than (6.26), showing that the enstrophy is dominantly contributed from the lower-wavenumber region  $k < k_d$ . It should be noted that the logarithmic divergence of the enstrophy does not affect the vanishing energy dissipation in the inviscid limit (3.5) which is characteristic of two-dimensional turbulence.

If we require the matching of the modified similarity law in the enstrophy-dissipation range with the inviscid similarity law (6.9), we obtain the same inertial subrange spectrum (6.24) with logarithmic correction terms of smaller order. Thus, there arises no need for substantial modification of the inertial subrange spectrum such as the logarithmic correction proposed by Kraichnan (1971). This is simply because Kraichnan's correction was introduced to make  $\eta$  finite, which he assumed in deriving the

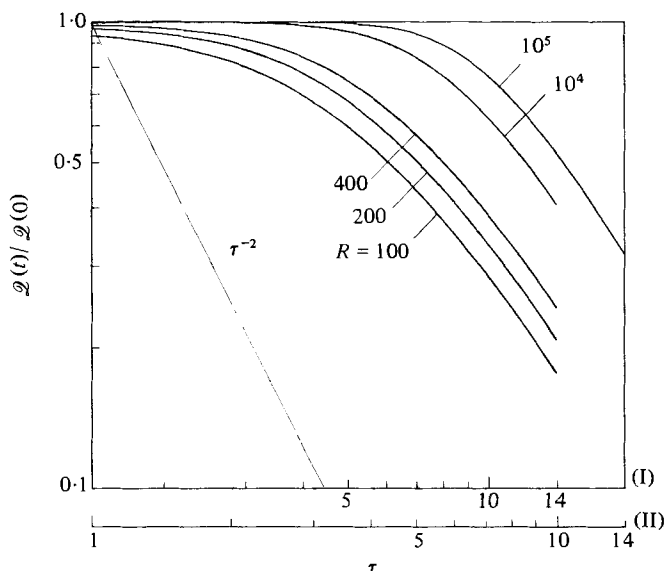


FIGURE 4. The decay of enstrophy  $\mathcal{Q}(t)$ . Case I,  $\mathcal{Q}(0)/(u_0 k_0)^2 = 1$ .  
Case II,  $\mathcal{Q}(0)/(u_0 k_0)^2 = 2$ .

inertial subrange spectrum (3.8), whereas a logarithmically divergent  $\eta$  is compatible with (3.8) or (6.24) in our theory.

According to Kraichnan's argument, the eddy-damping term is expressed as

$$\omega_k = \left( \int_0^k p^2 E(p) dp \right)^{\frac{1}{2}} \approx (\log R)^{\frac{1}{2}},$$

for  $k \approx k_d \approx R^{\frac{1}{2}} \gg 1$ , and the enstrophy dissipation or the total enstrophy transfer is given by

$$\eta \approx \omega_k k^3 E(k) = \text{const.}, \tag{6.30}$$

thanks to the correction factor  $(\log R)^{-\frac{1}{2}}$  in  $E(k)$ . If, on the other hand,  $\eta$  is calculated using the expression

$$\eta = \int_0^\infty \omega_k k^2 E(k) dk, \tag{6.31}$$

instead of (6.30), it would lead to the same divergent expression  $\eta \approx \log R$  as (6.27) in spite of the difference in the form of the logarithmic correction.

(v) *Far-dissipation range*

The asymptotic behaviour of the energy spectrum for extremely high wavenumbers can be obtained following the same procedure as that employed by Tatsumi & Kida (1980) for three-dimensional turbulence. The result is expressed as

$$E(k, t)/E_0 = 128 \cdot 3b^{\frac{3}{2}} R^{-\frac{1}{4}} \tau_*^{\frac{3}{4}} \kappa^{\frac{1}{2}} \exp[-b\kappa/(R^{\frac{1}{2}} \tau_*^{-\frac{1}{2}})], \tag{6.32}$$

where  $b$  is a constant.

The asymptotic behaviour of the numerically obtained spectrum (5.6) for very high wavenumbers is at variance with (6.32), but the discrepancy seems to be due to the insufficient accuracy of the numerical work.

## 7. Enstrophy

The enstrophy  $\mathcal{Q}(t)$  is calculated using the relation (2.7) and the numerical results of the energy spectrum. The results for  $R = 100, 200, 400, 10^4$  and  $10^5$  are shown graphically in figure 4. The striking feature of the results is that all curves (above  $R = 100$ ) for cases I and II can be made to overlap almost completely if the abscissa of case II is shifted by the amount  $1.4 \doteq \sqrt{2}$ .

This empirical law is accounted for as follows. In two-dimensional turbulence the evolution of the enstrophy-containing part of the energy spectrum is independent of the details of the spectrum at very low wavenumbers. Therefore the non-dimensional enstrophy  $\mathcal{Q}(t)/(u_0 k_0)^2$  will undergo a universal evolution

$$\mathcal{Q}(t)/(u_0 k_0)^2 = G(\tau), \quad (7.1)$$

irrespective of the initial condition of the energy spectrum at very low wavenumbers. According to the initial conditions (4.2) and (4.3),  $\mathcal{Q}(0)/(u_0 k_0)^2 = 1$  and  $2$  for cases I and II respectively. Hence, if we adopt a new characteristic scale  $(u_0 k_0)' = \sqrt{2}(u_0 k_0)$  for case II, the nondimensional enstrophy must follow the same evolution as (7.1),

$$\mathcal{Q}(t)/(u_0 k_0)'^2 = G(\tau'), \quad (7.2)$$

where

$$\tau' = (u_0 k_0)'t = \sqrt{2}\tau. \quad (7.3)$$

The empirical law now follows from the equivalence of (7.1) and (7.2) under the transformation (7.3).

Figure 4 shows that the enstrophy  $\mathcal{Q}(t)$  decreases monotonically in time. At very large Reynolds numbers,  $\mathcal{Q}(t)$  remains nearly constant during the initial period  $0 \leq t < t_c$ ,  $t_c$  being a critical time, and then decreases in the later period  $t > t_c$ . An analogous trend was observed in three-dimensional turbulence (see André & Lesieur 1977, Tatsumi & Kida 1980), where the decay of energy  $\mathcal{E}(t)$  starts almost discontinuously at  $t_c$ , which is nearly constant at very large Reynolds numbers. In two-dimensional turbulence, on the other hand, the change in  $\mathcal{Q}(t)$  around  $t_c$  is more gradual and  $t_c$  increases with Reynolds number roughly in proportion to  $(\log R)^{\frac{1}{2}}$ .

The similarity law (6.26) for the evolution of the enstrophy is expressed as

$$\mathcal{Q}(t) \propto \tau_{**}^{-2}, \quad (7.4)$$

with

$$\tau_{**} = \tau (\log R\tau)^{-\frac{1}{2}}. \quad (7.5)$$

The validity of this law is checked by plotting the numerical curves of  $\mathcal{Q}(t)$  in terms of the time  $\tau_{**}$  as shown in figure 5. The curves appear to approach fairly closely the asymptotic line (7.4) as  $R$  and  $\tau$  tend to infinity, but the lengths of the numerical curves are not sufficient to confirm the approach decisively. The best fit for the asymptotic law is obtained by the extrapolation of the curves as

$$\frac{\mathcal{Q}(t)}{\mathcal{Q}(0)} = \begin{cases} 1 & \text{for } \tau_{**} < \tau_{**c}, \\ (\tau_{**}/\tau_{**c})^{-2} & \text{for } \tau_{**} > \tau_{**c}, \end{cases} \quad (7.6)$$

with  $\tau_{**c} = 3.32$  and  $2.37$  ( $\doteq 3.32/\sqrt{2}$ ) for cases I and II respectively. The transformation law (7.3) is also observed in this presentation.



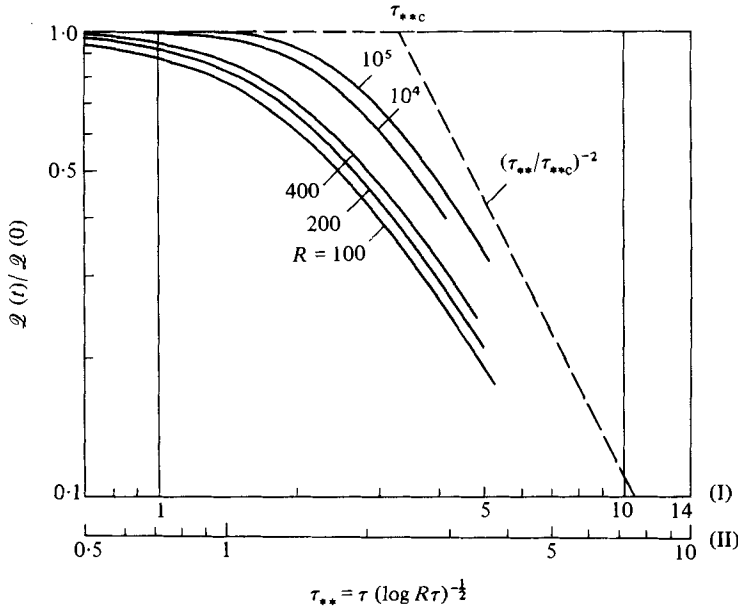


FIGURE 5. The similarity of the decay of enstrophy  $\mathcal{Q}(t)$ .  $\tau_{**} = \tau(\log R\tau)^{-\frac{1}{2}}$ .

The asymptotic law (7.6) shows that the enstrophy dissipation takes place in the period  $\tau_{**} > \tau_{**c}$ , that is, in view of (7.5) and (4.1),

$$t > (u_0 k_0)^{-1} \tau_{**c} (\log R)^{\frac{1}{2}} \tag{7.7}$$

for large  $R$ . This relation is shown to be consistent with the inequality (3.9) given by Pouquet *et al.* (1975). According to (3.2), the palinstrophy  $\mathcal{P}$  must be  $O(1/\nu) = O(R)$  in order to make the enstrophy dissipation  $\eta$  non-zero in the limit of  $R \rightarrow \infty$ . Then, it follows from (3.9) that

$$\exp[\frac{1}{2} \mathcal{Q}(0) t^2] > O(R),$$

that is,

$$t > O((\log R)^{\frac{1}{2}}), \tag{7.8}$$

which is in complete agreement with (7.7).

As will be shown in §8 below, the time similarity of the second-order cumulant derived under the present approximation is not changed by taking account of the higher-order cumulants. Therefore the time similarity of the enstrophy (7.4) or (7.6) is also unchanged, and represents an exact result independent of any closure approximation although the numerical value of  $\tau_{**c}$  in (7.6) may depend upon the approximation employed.

### 8. Similarity of higher-order cumulants and characteristic functional

In this section, we attempt to generalize the similarity laws of the energy spectrum obtained under the modified zero fourth-cumulant approximation to higher-order cumulants and thus to show that these similarity laws are exact results which are free from any closure assumption.

The cumulants are defined as the coefficients of the logarithmic Taylor expansion of the characteristic functional  $\Phi$ :

$$\Phi[z(\mathbf{k}), t] = \exp [W(z, t)]. \tag{8.1}$$

$$W(z, t) = \sum_{n=2}^{\infty} \frac{i^n}{n!} \int \dots \int C^{(n)}(\mathbf{k}_1, \dots, \mathbf{k}_n, t) \delta(\mathbf{k}_1 + \dots + \mathbf{k}_n) z(\mathbf{k}_1) \dots z(\mathbf{k}_n) d\mathbf{k}_1 \dots d\mathbf{k}_n, \tag{8.2}$$

where  $C^{(n)}$  denotes the  $n$ th-order cumulant. Substitution of the expansion (8.2) into equation (2.3) gives an infinite set of equations for the cumulants, which may be written in symbolic manner as

$$\left. \begin{aligned} \left(\frac{\partial}{\partial t} + \nu k^2\right) C^{(2)} &= \int C^{(3)} d\mathbf{h}, \\ \left(\frac{\partial}{\partial t} + \nu k^2\right) C^{(3)} &= \int C^{(4)} d\mathbf{h} + C^{(2)}C^{(2)}, \\ &\vdots \\ \left(\frac{\partial}{\partial t} + \nu k^2\right) C^{(n)} &= \int C^{(n+1)} d\mathbf{h} + \sum_{r=2}^{n-1} C^{(r)}C^{(n-r+1)}. \end{aligned} \right\} \tag{8.3}$$

(i) *Energy-containing range*

According to the similarity law (6.9),

$$C^{(2)} \simeq kE(k) = O(1), \tag{8.4}$$

in the energy-containing range. Then, it may be obvious that the set of equations (8.3) is satisfied by the cumulants of the following orders in this range:

$$C^{(n)} = O(t^{n-2}), \quad n = 2, 3, \dots \tag{8.5}$$

The similarity law of the cumulants (8.5) can be expressed in terms of the characteristic functional. In view of (6.9) and (8.5), we may write

$$\mathbf{k} = t^{-1}\mathbf{q}, \tag{8.6}$$

$$C^{(n)} = t^{n-2} \Gamma^{(n)}, \tag{8.7}$$

where the reduced wavenumber  $\mathbf{q}$  and cumulants  $\Gamma^{(n)}$  are assumed to be of order one. Then, (8.2) is written as

$$W(z, t) = \sum_{n=2}^{\infty} \frac{i^n}{n!} t^{-n} \int \dots \int \Gamma^{(n)}(\mathbf{q}_1, \dots, \mathbf{q}_n, t) \delta(\mathbf{q}_1 + \dots + \mathbf{q}_n) z(\mathbf{q}_1) \dots z(\mathbf{q}_n) d\mathbf{q}_1 \dots d\mathbf{q}_n. \tag{8.8}$$

The presence of the  $t^{-n}$  factor in the  $n$ th-order term seems to suggest rapid convergence of the cumulant series (8.8) in time. It should be noted, however, that this fact does not necessarily imply the validity of the central limit theorem for  $t \rightarrow \infty$ . If we introduce a new argument function,

$$\zeta(\mathbf{q}) = t^{-1} z(\mathbf{k}), \tag{8.9}$$

in order to make the second-order term independent of time, we find that all other terms also become time-independent. Thus, although the higher-order cumulants are of smaller order with respect to  $t^{-1}$  in the energy-containing range, they are just in balance with each other in the cumulant equations (8.3) and give contributions of the

same order to the characteristic functional. The invalidity of the central limit theorem in the energy-containing range is at variance with the general belief in normality of the large-scale components of turbulence, which has been experimentally established for three-dimensional turbulence (see, for instance, Van Atta & Chen 1968).

(ii) *Enstrophy-dissipation range*

The similarity law of the energy spectrum in the enstrophy-dissipation range is given by (6.21). Then, following the same procedure as in (i), we find that the set of equations (8.3) is satisfied by the cumulants of the following orders in this range:

$$C^{(n)} = O(R^{1-n}t^{-1}). \quad (8.10)$$

Thus, for large values of the Reynolds number and time, the cumulant  $C^{(n)}$  decreases monotonically as the order  $n$  increases.

The similarity law of the cumulants (8.10) can also be expressed in terms of the characteristic functional. In view of (6.20) and (8.10), we may put

$$\mathbf{k} = R^{\frac{1}{2}}t^{-\frac{1}{2}}\mathbf{q}, \quad C^{(n)} = R^{-(n-1)}t^{-1}\Gamma^{(n)}, \quad (8.11)$$

where  $\mathbf{q}$  and  $\Gamma^{(n)}$ 's are again quantities of order unity. Then, we obtain the same expression as (8.8) and hence find, through the transformation (8.9), that all terms are of the same order in this range. The invalidity of the central limit theorem is not unexpected in the enstrophy-dissipation range since the nonlinear interaction associated with finite enstrophy transfer is supposed to produce strong non-Gaussian character of small-scale components of turbulence.

(iii) *Statistical quantities determined by the similarity laws*

It has been established that the similarity laws for the energy spectrum in the energy-containing and enstrophy-dissipation ranges obtained above are exact results independent of any closure approximation. This conclusion indicates that the statistical quantities which are determined solely by these similarity laws also represent exact results. Thus, for instance, the dependence on Reynolds number and time of the enstrophy  $\mathcal{Q}$  ((6.10), (6.23)), the enstrophy dissipation  $\eta$  ((6.11), (6.22)) and the inertial subrange spectrum ((3.8), (6.24)) can be taken to be exact (not necessarily unique) results, but the numerical coefficients associated with these quantities are not final and are likely to be affected by higher-order approximations.

## 9. Comparison with numerical experiments

Numerical experiments on two-dimensional turbulence have been carried out by several authors. Lilly (1969, 1971) solved the vorticity equation (2.1) numerically in a square domain with periodic boundaries using the difference method with 64 mesh points and obtained the energy spectrum of the  $k^{-3}$  form. On the other hand, Deem & Zabusky (1971) obtained the  $k^{-4}$  spectrum using nearly the same numerical method. These earlier results were, however, shown to be inconclusive by Herring *et al.* (1974) who carried out a numerical calculation using both the finite difference and spectral methods with 64 and 128 mesh points. Since the spectral curves due to the finite difference method with 64 mesh points are found to change considerably by doubling the mesh points, conclusions concerning the spectrum based on the calculation with

64 mesh points are unreliable. According to the results of Herring *et al.* based on the spectral method with 128 mesh points, the spectrum takes the  $k^{-4}$  form at the highest Reynolds number employed  $R = 1184$ , or  $R = 973$  by our definition. It is reported, however, by Orszag (1978) that the  $k^{-3}$  spectrum has been attained by the numerical calculation at much higher Reynolds number  $R = 25\,500$ , or  $R = 9728$  by our definition.

Fornberg (1977) solved the inviscid vorticity equation numerically using the spectral method with 64 mesh points and introducing a dissipative effect by discarding all modes with wavenumbers  $> 20$  at every 60 time steps. According to his results, the spectrum takes the  $k^{-3}$  form in the earlier period of evolution ( $t < 1000$  in an arbitrary unit) and then the  $k^{-4}$  form in the far-later period ( $t > 3000$ ). It is observed from the picture display of the iso-vorticity lines that the stretching of these lines produces regions of high vorticity-gradient in the earlier period while the far-later period is characterized by the formation of well-defined vortex regions separated from each other.

The generation of high vorticity gradients or large palinstrophy  $\mathcal{P}$  in the earlier period leads to a finite enstrophy dissipation  $\eta > 0$  and is compatible with the appearance of the  $k^{-3}$  spectrum in this period. In the far-later period, on the other hand, the formation of separated vortex regions, which is equivalent to the build-up of the phase relations between different wavenumber components, accounts for the vanishing enstrophy transfer and the absence of the  $k^{-3}$  spectrum in the later period. The affinity of the vorticity field of the far-later period with the piece-wise continuous distribution of vorticity assumed by Saffman (1971) gives good reason for the closeness of the numerical results with the  $k^{-4}$  spectrum predicted by him.

Finally, it should be noted that the two-dimensional Euler equation, or equation (2.1) with  $\nu \equiv 0$ , was investigated mathematically by Kato (1967) and Sulem (1978), and it was concluded that the solution remains regular if it is so initially. Apparently this conclusion excludes the possibility of singular behaviour of the solution in the inviscid limit  $\nu \rightarrow 0$ . On the other hand, our result shows that the palinstrophy  $\mathcal{P}$  increases indefinitely as  $O(\nu^{-1})$  in this limit. This result, however, is not in conflict with the above-mentioned regularity of the inviscid two-dimensional flows since the commencement of divergence of the palinstrophy is delayed indefinitely as  $t_c \propto (\log \nu^{-1})^{\frac{1}{2}}$  in the inviscid limit.

A part of the present work was reported in the Euromech Symposium on 'Two-dimensional and quasi-two-dimensional turbulence' held on 5–9 September 1978 at Grenoble, France. Fruitful discussions with Dr Uriel Frisch, Dr Marcel Lesieur and other participants are kindly acknowledged. The authors' thanks are also due to Dr Shigeo Kida for his helpful comments. During the course of this work the authors have been in receipt of the Grants in Aid for Scientific Research from the Ministry of Education.

#### REFERENCES

- ANDRÉ, J. C. & LESIEUR, M. 1977 Influence of helicity on the evolution of isotropic turbulence at high Reynolds number. *J. Fluid Mech.* **81**, 187–207.
- BASDEVANT, C., LESIEUR, M. & SADOURNY, R. 1978 Subgrid modelling of enstrophy transfer in two-dimensional turbulence. *J. Atmos. Sci.* **6**, 1028–1042.
- BASDEVANT, C. & SADOURNY, R. 1975 Ergodic properties of inviscid truncated models of two-dimensional incompressible flows. *J. Fluid Mech.* **69**, 673–688.

- BATCHELOR, G. K. 1969 Computation of the energy spectrum in homogeneous two-dimensional turbulence. *Phys. Fluids Suppl.* **12**, II 233–239.
- BRISSAUD, A., FRISCH, U., LÉORAT, J., LESIEUR, M., MAZURE, A., POUQUET, A., SADOURNY, R. & SULEM, P. L. 1973 Catastrophe énergétique et nature de la turbulence. *Annales de Géophysique* **29**, 539–546.
- DEEM, G. S. & ZABUSKY, N. J. 1971 Ergodic boundary in numerical simulations of two-dimensional turbulence. *Phys. Rev. Lett.* **27**, 396–399.
- FJØRTOFT, R. 1953 On the changes in the spectral distribution of kinetic energy for two-dimensional, non-divergent flow. *Tellus* **5**, 225–230.
- FORNBERG, B. 1977 A numerical study for 2-D turbulence. *J. Comp. Phys.* **25**, 1–31.
- FOX, D. G. & ORSZAG, S. A. 1973 Inviscid dynamics of two-dimensional turbulence. *Phys. Fluids* **16**, 169–171.
- HERRING, J. R., ORSZAG, S. A., KRAICHNAN, R. H. & FOX, D. G. 1974 Decay of two-dimensional turbulence. *J. Fluid Mech.* **66**, 417–444.
- KATO, T. 1967 On the classical solutions of the two-dimensional non-stationary Euler equation. *Arch. Rat. Mech. Anal.* **25**, 188–200.
- KELLS, L. C. & ORSZAG, S. A. 1978 Randomness of low-order models of two-dimensional inviscid dynamics. *Phys. Fluids* **21**, 162–168.
- KRAICHNAN, R. H. 1967 Inertial ranges in two-dimensional turbulence. *Phys. Fluids* **10**, 1417–1423.
- KRAICHNAN, R. H. 1971 Inertial-range transfer in two- and three-dimensional turbulence. *J. Fluid Mech.* **47**, 525–535.
- KRAICHNAN, R. H. 1975 Statistical dynamics of two-dimensional flow. *J. Fluid Mech.* **67**, 155–175.
- KRAICHNAN, R. H. & MONTGOMERY, D. 1979 Two-dimensional turbulence. Preprint.
- LEITH, C. E. 1968 Diffusion approximation for two-dimensional turbulence. *Phys. Fluids* **11**, 671–673.
- LEITH, C. E. 1971 Atmospheric predictability and two-dimensional turbulence. *J. Atmos. Sci.* **28**, 145–161.
- LEITH, C. E. & KRAICHNAN, R. H. 1972 Predictability of turbulent flows. *J. Atmos. Sci.* **29**, 1041–1058.
- LESIEUR, M. & SCHERTZER, D. 1978 Amortissement autosimilaire d'une turbulence à grand nombre de Reynolds. *Mécanique* **17**, 609–646.
- LILLY, D. K. 1969 Numerical simulation of two-dimensional turbulence. *Phys. Fluids Suppl.* **12**, II 240–249.
- LILLY, D. K. 1971 Numerical simulation of developing and decaying two-dimensional turbulence. *J. Fluid Mech.* **45**, 395–415.
- OGURA, Y. 1962 Energy transfer in a normally distributed and isotropic turbulent velocity field in two dimensions. *Phys. Fluids* **5**, 395–401.
- ONISAGER, L. 1949 Statistical hydrodynamics. *Nuovo Cimento Suppl.* **6**, 279–287.
- ORSZAG, S. A. 1977 Lectures on the statistical theory of turbulence. *Fluid Dynamics: Les Houches 1973* (eds R. Balian & J. L. Peube). Gordon & Breach.
- ORSZAG, S. A. 1978 Turbulence and transition: A progress report. Private communication.
- POUQUET, A., LESIEUR, M., ANDRÉ, J. C. & BASDEVANT, C. 1975 Evolution of high Reynolds number two-dimensional turbulence. *J. Fluid Mech.* **72**, 305–319.
- PROUDMAN, I. & REID, W. H. 1954 On the decay of normally distributed and homogeneous turbulent velocity field. *Phil. Trans. Roy. Soc. A* **247**, 163–189.
- SAFFMAN, P. G. 1971 On the spectrum and decay of random two dimensional vorticity distributions. *Studies in Appl. Math.* **50**, 377–383.
- SEYLER, C. E., SALU, Y., MONTGOMERY, D. & KNORR, G. 1975 Two-dimensional turbulence in inviscid fluids or guiding center plasmas. *Phys. Fluids* **18**, 803–813.
- SULEM, C. 1978 Régularité globale d'un fluide parfait occupant une bande de  $R^2$ , pour des données initiales non nulles à l'infini. Private communication.

- TATSUMI, T. & KIDA, S. 1980 The modified cumulant expansion for isotropic turbulence at large Reynolds numbers. *J. Phys. Soc. Japan* **49**, 2014–2025.
- TATSUMI, T., KIDA, S. & MIZUSHIMA, J. 1978 The multiple-scale cumulant expansion for isotropic turbulence. *J. Fluid Mech.* **85**, 97–142.
- VAN ATTA, C. W. & CHEN, W. Y. 1968 Correlation measurements in grid turbulence using digital harmonic analysis. *J. Fluid Mech.* **34**, 497–515.